Quantum-to-Classical Crossover in Many-Body Chaos and Scrambling from Relaxation in a Glass

Surajit Bera,[1,*] K. Y. Venkata Lokesh,[2,†] and Sumilan Banerjee[1,‡]
[1]Centre for Condensed Matter Theory, Department of Physics, Indian Institute of Science, Bangalore 560012, India
[2]Centre of High Energy Physics, Indian Institute of Science, Bangalore 560012, India

(Received 29 June 2021; accepted 23 February 2022; published 18 March 2022)

Chaotic quantum systems with Lyapunov exponent λ_L obey an upper bound $\lambda_L \leq 2\pi k_B T/\hbar$ at temperature T, implying a divergence of the bound in the classical limit $\hbar \to 0$. Following this trend, does a quantum system necessarily become "more chaotic" when quantum fluctuations are reduced? Moreover, how do symmetry breaking and associated nontrivial dynamics influence the interplay of quantum mechanics and chaos? We explore these questions by computing $\lambda_L(\hbar, T)$ in the quantum spherical p-spin glass model, where $\hbar$ can be continuously varied. We find that quantum fluctuations, in general, make paramagnetic phase less and the replica symmetry-broken spin glass phase more chaotic. We show that the approach to the classical limit could be nontrivial, with nonmonotonic dependence of λ_L on $\hbar$ close to the dynamical glass transition temperature T_d. Our results in the classical limit ($\hbar \to 0$) naturally describe chaos in supercooled liquid in structural glasses. We find a maximum in $\lambda_L(T)$ substantially above T_d, concomitant with the crossover from simple to slow glassy relaxation. We further show that $\lambda_L \sim T^\alpha$, with the exponent α varying between 2 and 1 from quantum to classical limit, at low temperatures in the spin glass phase.

DOI: 10.1103/PhysRevLett.128.115302

Understanding thermalization and transport rates in many-body systems and how quantum mechanics affects these rates across various phases and phase transitions have important implications for a remarkably wide range of topics. These include information scrambling in black holes [1,2] and quantum circuits [3], strange metals and Planckian dissipation [4,5], and complex dynamics in disordered systems [6,7]. Recently a quantum Lyapunov exponent or scrambling rate λ_L [8] has emerged as one of the important diagnostics of thermalization for several important systems [2,9–12] in high-energy and condensed matter physics. Quantum mechanics fundamentally influences this quantity by setting an upper bound $\lambda_L \leq 2\pi k_B T/\hbar$ [2] for a system at temperature T.

However, typically the Lyapunov exponent can only be extracted for quantum systems with a suitable semiclassical limit [2,9–12]. An important class of models for such systems corresponds to the solvable large-N Sachdev-Ye-Kitaev (SYK) model [9,10,13] and its variants [14–18], where λ_L can be calculated exactly in the large-N semiclassical limit. Nevertheless, once this limit is taken, no other quantum parameter like "$\hbar$" can be tuned in the SYK-type models to explore how quantum mechanics actually intervenes in the evolution of chaos between the classical and quantum limits. Also these models typically do not exhibit any symmetry breaking phase transitions and associated nontrivial dynamics. To address these, we study many-body chaos in one of the most studied solvable models of glasses, namely, the spherical p-spin glass model [19–28]. We show that the p-spin glass model gives us highly tunable analytical access to the interplay between chaos, quantum fluctuations, symmetry breaking, and complex dynamics.

We compute the Lyapunov exponent in the quantum p-spin glass model [22–27] of N spins interacting with random all-to-all p-spin interactions. The model shares many common features with other models of quantum spin glass, like transverse-field models [29–32]. Unlike the latter, the quantum p-spin glass model is solvable both in the classical and quantum limits for $N \to \infty$. Moreover, the dynamics of the model in the classical limit $\hbar \to 0$ is of great importance for structural glasses [6] and is identical to the mode coupling theory (MCT) dynamics in supercooled liquids [33–35]. As shown in Fig. 1, the model has thermodynamic transition, $T_c(\hbar)$, between paramagnetic (PM) and replica-symmetry broken (RSB) spin glass (SG) phase for $p \geq 3$ [26,27]. There is a dynamical transition at $T_d > T_c$ from slow glassy thermalization to lack of ergodicity below T_d and a relaxation time τ_α, extracted from spin-spin correlation function, diverges for $T \to T_d^+$.

We obtain $\lambda_L(\hbar, T)$ from the out-of-time-ordered correlator (OTOC) [2,8] for the quantum spin glass by varying $\hbar$ over the entire phase diagram (Fig. 1), with the following main results. (1) We show that quantum fluctuations, in general, reduce chaos in the disordered phase (PM) and increase chaos in the ordered (SG) phase. However, we find that λ_L, over certain temperature range close to $T_d(\hbar)$ in the PM phase, is a nonmonotonic function of $\hbar$. This indicates

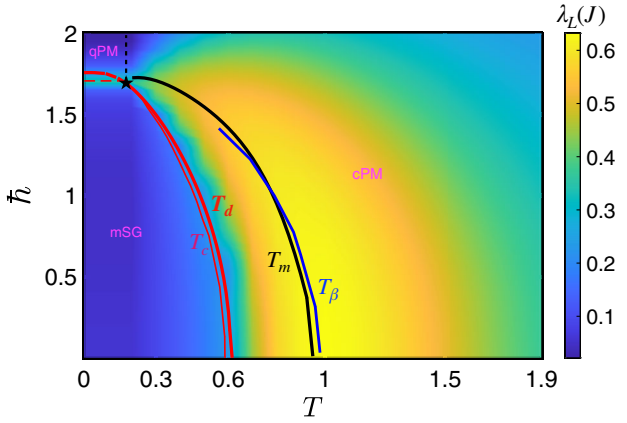

FIG. 1. Lyapunov exponent $\lambda_L(\hbar, T)$ (color map, in units of J) on the thermodynamic phase diagram. The thermodynamic PM-SG phase transition $T_c(\hbar)$ line (thin red solid line) is second order up to a tricritical point (black star) and then first order (thin dashed red line). The mSG to PM transition is demarcated by the dynamical transition line $T_d(\hbar) > T_c(\hbar)$ (thick solid red line). The locus of the broad maximum of $\lambda_L(T, \hbar)$ is shown as $T_m(\hbar)$ line (solid black line) and compared with the crossover temperature $T_\beta(\hbar)$ to the two-step glassy relaxation regime (blue line).

nontrivial nature of quantum corrections to λ_L. (2) By taking $\hbar \to 0$ limit for $T > T_d$, we obtain the temperature dependence of the Lyapunov exponent of a supercooled liquid. (3) We show that, unlike τ_α, λ_L^{-1} has a broad minimum at $T = T_m > T_d$ (Fig. 1), correlated with the crossover to the two-step glassy relaxation [33–35]. We analytically show that T_m signifies a crossover in chaos, arising due to an interplay of relaxation, the rapid increase of relaxation time in the glassy regime, and the crossover from strong coupling ($\gtrsim T$) to weak coupling ($\lesssim T$). This result is more general than the model considered here and should have implications for complex relaxations in liquids and many other interacting systems. (4) For λ_L in the SG phase, we obtain the OTOC in a replica-symmetry broken marginal SG (mSG) phase [26,27]. We find $\lambda_L \sim T^\alpha$ at low temperature in the mSG phase, with the exponent α varying between $\sim 2 - 1$ from quantum to the classical limit.

Earlier works [36,37] have studied chaos in the PM phase of a quantum rotor glass model [38] with two-rotor interaction. The model has the same thermodynamic phase diagram as the $p = 2$ spin glass model and the SG phase is replica symmetric [39]. A similar SG phase is also realized in a version of the SYK model represented in terms of SO (N) spins, where the Lyapunov exponent has been computed via numerical simulation in the classical large spin limit [40]. In this Letter we provide the first calculation of quantum OTOC and the associated Lyapunov exponent via Schwinger-Keldysh methods, from the quantum to classical limit, in the $p = 3$ spin glass model. The model exhibits a nontrivial replica symmetry broken SG phase and a complex glassy relaxation regime unlike the models considered in the previous studies [36,37,40].

Model.—We study the quantum spherical p-spin glass model [24–27], described by the Hamiltonian,

$$\mathcal{H} = \sum_i \frac{\pi_i^2}{2M} + \sum_{p, i_1 < \ldots < i_p} J^{(p)}_{i_1 \ldots i_p} s_{i_1} \ldots s_{i_p}, \tag{1}$$

with random all-to-all interactions among $p = 2, 3, \ldots$ spins on $i = 1, \ldots, N$ sites; the couplings $J^{(p)}_{i_1 \ldots i_p}$ s drawn from Gaussian distribution with variance $J_p^2 p!/2N^{p-1}$. The quantum dynamics results from the commutation relation $[s_i, \pi_j] = \mathrm{i}\hbar\delta_{ij}$. The model is nontrivial due to the spherical constraint $\sum_i s_i^2 = N$. The Hamiltonian describes a particle with mass M moving on the surface of an N-dimensional hypersphere. We study chaos in the model with $p = 3$ ($J_3 = J$). For $p = 2$, the model is noninteracting [39] and nonchaotic, i.e., $\lambda_L = 0$.

Large-N saddle points and phase diagram.—The equilibrium and dynamical phase diagrams of the model [Eq. (1)] have been analyzed in detail [22–27,41]. In the $N \to \infty$ limit, the phases are characterized by disorder averaged time-ordered ($\mathcal{T}_\tau$) correlation function, $Q_{ab}(\tau) = (1/N)\sum_i \langle \mathcal{T}_\tau s_{ia}(\tau) s_{ib}(0)\rangle$, obtained from the saddle point equations of the imaginary time (τ) path integral (see Supplemental Material, Sec. S1 [42]),

$$Q^{-1}_{ab}(\omega_k) = \left(\frac{\omega_k^2}{\Gamma} + z\right)\delta_{ab} - \Sigma_{ab}(\omega_k) \tag{2a}$$

$$\Sigma_{ab}(\tau) = \sum_p \frac{p\tilde{J}_p^2}{2}[Q_{ab}(\tau)]^{p-1}. \tag{2b}$$

The replicas $a = 1, \ldots, n$ are introduced to perform the disorder averaging and $\omega_k = 2k\pi T$ is bosonic Matsubara frequency with k an integer ($k_B = 1$); $\tilde{J}_p = J_p/J$, and temperature, time, and frequency are in units of J, $\hbar/J$, and $J/\hbar$, respectively. $Q_{ab}(\omega_k) = \int_0^\beta d\tau e^{\mathrm{i}\omega_k \tau} Q_{ab}(\tau)$ ($\beta = 1/T$) is matrix in replica space and the spherical constraint, $(1/N)\sum_i s_{ia}^2 = Q_{aa}(\tau = 0) = 1$, is imposed via the Lagrange multiplier z. The quantum fluctuations is tuned through the dimensionless parameter $\Gamma = \hbar^2/MJ$ by changing $\hbar$ with fixed M [43].

As in the earlier works [26,27], we obtain the phase diagram (Fig. 1) by numerically solving the saddle-point equations [Eqs. (2)] (see Supplemental Material, Secs. S1 1, S1 3 [42]). The replica structure of $Q_{ab}(\tau)$ for $n \to 0$ characterizes PM and SG phases, namely, (a) in the *PM phase*, $Q_{ab}(\tau) = Q(\tau)\delta_{ab}$ is replica symmetric, and (b) for the *SG phase*, the order parameter has an exact one-step replica symmetry breaking (1-RSB) structure where n replicas are broken into diagonal blocks with m replicas and $Q_{ab}(\tau) = [q_d(\tau) - q_{\mathrm{EA}}]\delta_{ab} + q_{\mathrm{EA}}\epsilon_{ab}$; $\epsilon_{ab} = 1$ if a, b are in diagonal block else $\epsilon_{ab} = 0$. The Edward-Anderson

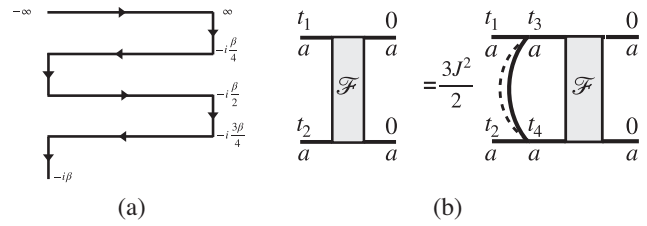

FIG. 2. (a) The four real-time branches (separated by imaginary time $\beta/4$) of the Schwinger-Keldysh contour used for computing the OTOC. (b) The ladder diagram for Eq. (3) for the $\mathcal{O}(1/N)$ term ($\mathcal{F}_a$) in the OTOC $F_a(t_1, t_2)$ is shown for $p = 3$. The solid horizontal lines denote the dressed retarded propagator $Q^R_{aa}(t_1, t_3)$, $Q^R_{aa}(t_2, t_4)$ and the vertical rung denotes the Wightmann function $Q^W_{aa}(t_3, t_4)$. The dotted line represents disorder averaging.

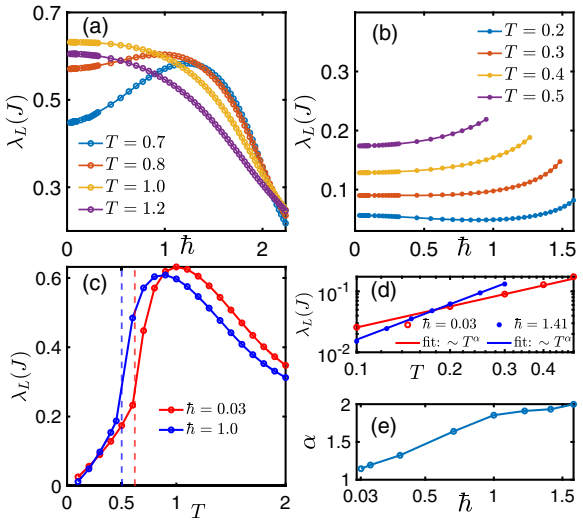

FIG. 3. (a) Lyapunov exponent λ_L (in units of J) as a function of $\hbar$ for several values of T in the cPM phase. (b) λ_L (in units of J) as a function of $\hbar$ for several values of T in the mSG phase. (c) $\lambda_L(T)$ (in units of J) across mSG-PM transitions [$T_d(\hbar)$, vertical dashed lines] for $\hbar = 0.03$, 1.0. (d) λ_L vs T (log-log scale) at low temperature for $\hbar = 0.03$, 1.41 fitted with a power-law $\lambda_L \propto T^\alpha$. (e) The exponent α varies from 1–2 as $\hbar$ varies from the classical limit to the quantum limit.

(EA) order parameter $q_{\rm EA}$ is finite in the SG phase and vanishes in the PM phase.

As shown in Fig. 1, the PM to SG phase transition $T_c(\hbar)$ is second order up to a tricritical point and then first order till $T = 0$ [26,27]. There are two PM phases, a classical PM (cPM), adiabatically connected to PM at $\hbar = 0$, and a quantum PM (qPM) phase for $T \lesssim T^*$ and above the first-order line. We compute λ_L in the cPM region since the qPM is strongly gapped [27], and hence very weakly chaotic. For the SG phase, we only consider the so-called marginal spin glass phase [27], where the block size or the break point m is obtained by the *marginal stability criterion* [27] (see Supplemental Material, Sec. S1 2 [42]). The mSG phase is demarcated by the dynamical phase transition line $T_d(\hbar) > T_c(\hbar)$ (Fig. 1).

For computing the Lyapunov exponent λ_L, we also need dynamical correlation and response functions in real time (frequency) t (ω). These are obtained using the spectral function $\rho(\omega) = -\mathrm{Im}Q^R_{aa}(\omega)/\pi$, where the retarded propagator, $Q^R_{ab}(\omega) = Q_{ab}(i\omega_k \to \omega + i0^+) = Q^R(\omega)\delta_{ab}$ (Supplemental Material, Sec. S1 1 [42]).

OTOC and the Lyapunov exponent.—As in the SYK model [9,44], the OTOC, $F(t) \sim \langle s_i(t)s_j(0)s_i(t)s_j(0)\rangle$ can be computed via real-time path integral method using a Schwinger-Keldysh (SK) contour with four branches, as shown in Fig. 2 [9,15,44]. However, in contrast to the SYK model, where the large-N saddle point is always replica symmetric [44], here we need to incorporate the nontrivial 1-RSB structure in the OTOC. We achieve this by using a replicated SK path integral [45,46] (Supplemental Material, Sec. S2 [42]). We define the following regularized disorder-averaged OTOC [2,44,47], $F_a(t_1, t_2) = (1/N^2)\sum_{ij}\mathrm{Tr}[ys_{ia}(t_1)ys_{ja}(0)ys_{ia}(t_2)ys_{ja}(0)]$, where $y^4 = \exp(-\beta H)/\mathrm{Tr}[\exp(-\beta H)]$. The Lyapunov exponent λ_L is extracted from the chaotic growth, $\mathcal{F}_a(t, t) \sim e^{\lambda_L t}$, that appears at $\mathcal{O}(1/N)$ in $F(t_1, t_2)$ (Supplemental Material, Sec. S2 1 [42]). Over the intermediate-time chaos regime, $\lambda_L^{-1} \lesssim t \lesssim \lambda_L^{-1}\ln(N)$, $\mathcal{F}_a(t_1, t_2)$ can be obtained from a Bethe-Salpeter-like equation [9,15,44],

$$\mathcal{F}_a(t_1, t_2) = \int dt_3 dt_4 K_a(t_1, t_2, t_3, t_4)\mathcal{F}_a(t_3, t_4). \quad (3)$$

The ladder kernel K, e.g., for $p = 3$, $K_a(t_1, t_2, t_3, t_4) = 3J^2 Q^R_{aa}(t_{13})Q^R_{aa}(t_{24})Q^W_{aa}(t_{34})$ $(t_{13} = t_1 - t_3)$ (see Supplemental Material, Sec. S2 1 [42]), is obtained using the retarded, $Q^R_{aa}(t)$, and the Wightmann, $Q^W_{aa}(t) = Q_{aa}(\tau \to it + \beta/2)$, correlators [47]. For the chaotic growth regime, using the ansatz $F_a(t_1, t_2) = e^{\lambda_L(t_1+t_2)/2} f_a(t_1 - t_2)$ [9,15,44], λ_L is obtained by numerically diagonalizing the kernel K (Supplemental Material, Sec. S2 2 [42]).

The information about the PM and SG phases are encoded in the ladder kernel and a crucial difference is in the Wightmann correlator, namely, for the SG phase $Q^W_{aa}(\omega) = \{2\pi\delta(\omega)q_{\rm EA} - [\pi\rho(\omega)/\sinh(\beta\omega/2)]\}$, whereas the first term is absent for Q^W in the PM phase, where $q_{\rm EA} = 0$.

Chaos in the paramagnetic phase.—We first discuss the dependence of λ_L on T and $\hbar$ in the cPM phase, as shown through the color map in Fig. 1 for $p = 3$. Overall, λ_L becomes small when T or $\hbar$ are large. λ_L exhibits a broad maximum at $T_m(\hbar)$, substantially above T_d, albeit tracking $T_d(\hbar)$ line and merging with it at the tricritical point. λ_L is plotted in Fig. 3(a) as function of $\hbar$ for several temperatures. For high and intermediate temperatures ($T \gtrsim J$), λ_L is a

monotonically decreasing function of $\hbar$, approaching a constant value in the classical limit $\hbar \to 0$. λ_L decreases rapidly for $\hbar \gtrsim 1$ since the system acquires a large spectral gap $\sim\Gamma$ for strong quantum fluctuations $\Gamma \gg T, J$ [27] (Supplemental Material, Sec. S4 2 [42]), making the interaction effects, and thus the chaos, very weak ($\lambda_L \sim e^{-\Gamma/T}$).

Remarkably, when temperature is close to $T_d(0)$, λ_L is a nonmonotonic function of $\hbar$. This implies that the approach to classical limit could be nontrivial for chaotic properties. A nonmonotonic dependence is also seen with T [Fig. 3(c)]. Starting from $T \gtrsim T_d(\hbar)$, λ_L initially increases reaching the maximum at T_m and then decreases with increasing T, as $\sim 1/T^2$ at high temperature $T \gg J$ (Supplemental Material, Sec. S4 1 [42]). In this limit, the system has a small gap $\sim\sqrt{\Gamma T} < T$ for $T > \Gamma$, whereas in the intermediate regimes $T, \Gamma \gtrsim T_m$, the system is soft gapped and becomes gapless in the classical limit $\Gamma \to 0$ (Supplemental Material, Sec. S3 [42]).

Chaos in the spin glass phase.—In contrast to the PM phases, the mSG phase is gapless [26,27]. Moreover, unlike that in the cPM phase [Fig. 3(a)], $\lambda_L(\hbar)$, in general, monotonically increases with $\hbar$, as shown in Fig. 3(b), apart from some weak nonmonotonic dependence on $\hbar$ at low temperatures. Thus, quantum fluctuations makes the system more chaotic in the mSG phase. Figure 3(c) shows $\lambda_L(T)$ for two $\hbar$ values. The Lyapunov exponent follows a power-law temperature dependence, $\lambda_L \sim T^\alpha$, with exponent α varying from 2 to 1 [Figs. 3(d) and 3(e)] with decreasing $\hbar$, implying $\lambda_L \sim T$ in the classical limit. However, the prefactor of linear T is much smaller than $2\pi/\hbar$ corresponding to the bound (see Supplemental Material, Sec. S4 3 [42]).

The temperature dependence $\lambda_L \sim T^2$, for large $\hbar$ [Fig. 1] within the mSG phase, is similar to that in a Fermi liquid [15,48,49]. This T dependence in the mSG phase can be understood based on the observation that the self-consistent equations for the time-dependent part of $Q_{ab}(\tau)$ [Eq. (2)], and the kernel [Eq. (3)], in the presence of 1-RSB are equivalent to those in the PM phase of an effective model with both $p = 3$ ($J_3 = J$) and $p = 2$ ($J_2 = J\sqrt{3q_{EA}}$) terms in Eq. (1) (Supplemental Material, Sec. S2 1 [42]). Irrespective of the J_3/J_2 ratio, $p = 3$ term is irrelevant at low energy and can be treated perturbatively, with a Lagrange multiplier $z = 2J_2$ such that the system is gapless like in the mSG. In this case, as discussed in the Supplemental Material, Sec. S4 4 [42], the integral kernel equation in Eq. (3) can be converted into

$$\left(-\frac{1}{2}\frac{\partial^2}{\partial t^2} - \mathrm{sech}^2 t\right) f(t) = -\frac{1}{3}\left(\lambda_L \frac{J_2^3}{\pi J_3^2 T^2} + 1\right) f(t),$$

i.e., a one-dimensional Schrödinger equation with Pöschl-Teller potential, with well-known eigenvalues [50]. This leads to $\lambda_L \sim T^2/q_{\mathrm{EA}}^{3/2}$. The exponent $\alpha \simeq 2$ matches with numerically obtained value in Fig. 3(e) in the quantum limit for large $\hbar$, where $J_2 \propto \sqrt{q_{EA}}$ is weakly temperature dependent (Supplemental Material, Sec. S4 4 [42]). Since quantum fluctuations reduce the SG order parameter q_{EA} (Supplemental Material, Sec. S4 4 [42]), $\lambda_L \sim q_{\mathrm{EA}}^{-3/2}$ naturally explains the enhancement of chaos [Fig. 3(b)] due to $\hbar$.

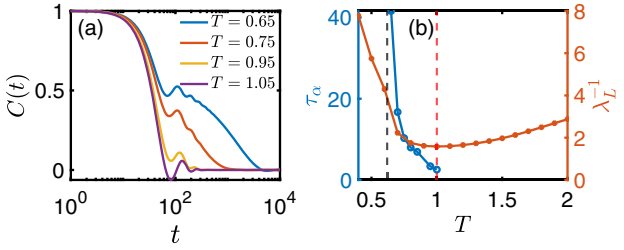

FIG. 4. (a) The correlation function $C(t)$ for several values of temperature T in the classical limit ($\hbar = \sqrt{0.001}$). (b) The α-relaxation timescale τ_α, diverging for $T \to T_d$ (vertical black dashed line), extracted from $C(t)$ and λ_L^{-1} as function of T in the classical limit $\hbar = \sqrt{0.001}$. The crossover temperature T_β to two-step β relaxation is shown by the vertical red-dashed line.

Scrambling from glassy relaxation.—As shown in Fig. 4(a), the decay of spin-spin correlation $C(t) = (1/N)\sum_i \langle s_i(t)s_i(0)$, becomes slower as $T \to T_d(\hbar)^+$. Moreover, close to T_d, $C(t)$ exhibits a two-step relaxation, typical characteristic of supercooled liquids [33–35], namely, (i) a fast microscopic decay followed by a slowly decaying plateaulike β-relaxation regime, and eventually (ii) the α regime with a stretched exponential decay $\sim \exp\left[-(t/\tau_\alpha)^{\beta_a}\right]$, with a diverging timescale $\tau_\alpha \sim (T - T_d)^{-\gamma}$ ($\gamma > 0$) and stretching exponent β_a [33–35]. The emergence of the two-step relaxation close to T_d is seen in Fig. 4(a) (Supplemental Material, Sec. S5 [42]). In Fig. 4(b), we plot τ_α extracted from the numerical fit to $C(t)$ [Fig. 4(a)] in the α regime and compare with λ_L^{-1}. In contrast to τ_α, λ_L^{-1} has a minimum at T_m, substantially above T_d. In Supplemental Material, Sec. S6 1 [42], we show that the stretched exponential part from α relaxation of $C(t)$ [Fig. 4(a)] alone with the τ_α shown in Fig. 4(b) give rise to the nonmonotonic $\lambda_L(T)$ [Fig. 3(c)]. We analytically solve the kernel equation [Eq. (3)] and obtain $\lambda_L(T)$ in the PM phase for Debye relaxation $\sim \exp(-t/\tau_\alpha)$ (Supplemental Material, Sec. S6 2 [42]). We show that

$$\lambda_L \sim \tau_\alpha^{-1}(2J/T - 1),$$

for $T \lesssim J$, leading to a maximum at $T_m \sim \sqrt{JT_d}$ for $\gamma = 1$. Thus, for temperature close to T_d, $\lambda_L \propto \tau_\alpha^{-1}$, i.e., the scrambling rate is controlled by relaxation rate. However, the crossover from strong ($J > T$) to weak ($J < T$) coupling in combination with the nontrivial temperature dependence of τ_α in the glassy regime, give rise to a crossover in chaos in the form of a maximum in the Lyapunov exponent. As shown in Fig. 1, we find that T_m is correlated with the crossover (T_β) to two-step glassy relaxation [Fig. 4(b)]. The onset of nontrivial temperature dependence of τ_α is presumably connected with

the onset of the two-step relaxation, leading to the correlation between T_m and T_β. However, to properly establish this relation, we need an analytical understanding of $C(t)$ and T_β, which is beyond the scope of this Letter.

Conclusions.—In this work, we have shown how quantum mechanics influences chaos in a solvable quantum spin glass model. We derive relation between chaos and relaxation rates in the complex glassy regime above the glass transition. So far, such direct relation between scrambling and relaxation has only been established for weakly interacting systems [11,12,15,47]. In future, studying the connection between many-body chaos and relaxation in simulation [51] of supercooled liquids [6] may lead to new insight into complex dynamics in glasses. It would be interesting to study the quantum to classical crossover in other models [40], where λ_L already starts at the upper bound $2\pi T/\hbar$ in the quantum limit. Also, the methods developed here to analyze chaos can be extended to transverse-field models [29–32], e.g., with Ising spins.

V. L. acknowledges support from CSIR, India. S. B. acknowledges support from SERB (ECR/2018/001742), DST, India.

Note added.—Recently, Ref. [52], which looks into a quantum p-spin glass model and its chaotic properties from the holographic perspective, appeared on arXiv.

*surajit@iisc.ac.in
†venkatakumar@iisc.ac.in
‡sumilan@iisc.ac.in

[1] Y. Sekino and L. Susskind, Fast scramblers, J. High Energy Phys. 10 (2008) 065.
[2] J. Maldacena, S. H. Shenker, and D. Stanford, A bound on chaos, J. High Energy Phys. 08 (2016) 106.
[3] P. Hosur, X. L. Qi, D. A. Roberts, and B. Yoshida, Chaos in quantum channels, J. High Energy Phys. 02 (2016) 004.
[4] J. A. N. Bruin, H. Sakai, R. S. Perry, and A. P. Mackenzie, Similarity of scattering rates in metals showing T-linear resistivity, Science **339**, 804 (2013).
[5] S. A. Hartnoll, Theory of universal incoherent metallic transport, Nat. Phys. **11**, 54 (2015).
[6] L. Berthier and G. Biroli, Theoretical perspective on the glass transition and amorphous materials, Rev. Mod. Phys. **83**, 587 (2011).
[7] D. A. Abanin, E. Altman, I. Bloch, and M. Serbyn, Colloquium: Many-body localization, thermalization, and entanglement, Rev. Mod. Phys. **91**, 021001 (2019).
[8] A. I. Larkin and Yu. N. Ovchinnikov, Quasiclassical method in the theory of superconductivity, Zh. Eksp. Teor. Fiz. **55**, 2262 (1968) [J. Exp. Theor. Phys. **28**, 1200 (1969)], http://jetp.ras.ru/cgi-bin/dn/e_028_06_1200.pdf.
[9] A. Kitaev, A simple model of quantum holography, in *Proceedings of the KITP, April 7, 2015 and May 27, 2015* (2015).
[10] A. Kitaev and S. J. Suh, Statistical mechanics of a two-dimensional black hole, J. High Energy Phys. 05 (2019) 198.
[11] I. L. Aleiner, L. Faoro, and L. B. Ioffe, Microscopic model of quantum butterfly effect: Out-of-time-order correlators and traveling combustion waves, Ann. Phys. (Amsterdam) **375**, 378 (2016).
[12] A. A. Patel, D. Chowdhury, S. Sachdev, and B. Swingle, Quantum Butterfly Effect in Weakly Interacting Diffusive Metals, Phys. Rev. X **7**, 031047 (2017).
[13] S. Sachdev, Bekenstein-Hawking Entropy and Strange Metals, Phys. Rev. X **5**, 041025 (2015).
[14] Y. Gu, X.-L. Qi, and D. Stanford, Local criticality, diffusion and chaos in generalized Sachdev-Ye-Kitaev models, J. High Energy Phys. 05 (2017) 125.
[15] S. Banerjee and E. Altman, Solvable model for a dynamical quantum phase transition from fast to slow scrambling, Phys. Rev. B **95**, 134302 (2017).
[16] R. A. Davison, W. Fu, A. Georges, Y. Gu, K. Jensen, and S. Sachdev, Thermoelectric transport in disordered metals without quasiparticles: The Sachdev-Ye-Kitaev models and holography, Phys. Rev. B **95**, 155131 (2017).
[17] S.-K. Jian, Z.-Y. Xian, and H. Yao, Quantum criticality and duality in the SYK/AdS_2 chain, Phys. Rev. B **97**, 205141 (2018).
[18] A. Haldar and V. B. Shenoy, Strange half-metals and Mott insulators in Sachdev-Ye-Kitaev models, Phys. Rev. B **98**, 165135 (2018).
[19] B. Derrida, Random-Energy Model: Limit of a Family of Disordered Models, Phys. Rev. Lett. **45**, 79 (1980).
[20] T. R. Kirkpatrick and D. Thirumalai, Dynamics of the Structural Glass Transition and the p-Spin—Interaction Spin-Glass Model, Phys. Rev. Lett. **58**, 2091 (1987).
[21] A. Crisanti and H. J. Sommers, The sphericalp-spin interaction spin glass model: The statics, Z. Phys. B Condens. Matter **87**, 341 (1992).
[22] Th. M. Nieuwenhuizen, Exactly Solvable Model of a Quantum Spin Glass, Phys. Rev. Lett. **74**, 4289 (1995).
[23] Th. M. Nieuwenhuizen, Quantum Description of Spherical Spins, Phys. Rev. Lett. **74**, 4293 (1995).
[24] L. F. Cugliandolo and G. Lozano, Quantum Aging in Mean-Field Models, Phys. Rev. Lett. **80**, 4979 (1998).
[25] L. F. Cugliandolo and G. Lozano, Real-time nonequilibrium dynamics of quantum glassy systems, Phys. Rev. B **59**, 915 (1999).
[26] L. F. Cugliandolo, D. R. Grempel, and C. A. da Silva Santos, From Second to First Order Transitions in a Disordered Quantum Magnet, Phys. Rev. Lett. **85**, 2589 (2000).
[27] L. F. Cugliandolo, D. R. Grempel, and C. A. da Silva Santos, Imaginary-time replica formalism study of a quantum spherical p-spin-glass model, Phys. Rev. B **64**, 014403 (2001).
[28] D. Facoetti, G. Biroli, J. Kurchan, and D. R. Reichman, Classical glasses, black holes, and strange quantum liquids, Phys. Rev. B **100**, 205108 (2019).
[29] Y. Y. Goldschmidt, Solvable model of the quantum spin glass in a transverse field, Phys. Rev. B **41**, 4858 (1990).
[30] V. Dobrosavljevic and D. Thirumalai, $1/p$ expansion for a p-spin interaction spin-glass model in a transverse field, J. Phys. A Math. Gen. **23**, L767 (1990).

[31] T. M. Nieuwenhuizen and F. Ritort, Quantum phase transition in spin glasses with multispin interactions, Physica (Amsterdam) **250A**, 8 (1998).
[32] T. Obuchi, H. Nishimori, and D. Sherrington, Phase diagram of the p-spin-interacting spin glass with ferromagnetic bias and a transverse field in the infinite- p limit, J. Phys. Soc. Jpn. **76**, 054002 (2007).
[33] W. Götze, *Complex Dynamics of Glass-Forming Liquids* (Oxford University Press, Oxford, 2008).
[34] W. Kob, The mode-coupling theory of the glass transition, arXiv:cond-mat/9702073.
[35] D. R. Reichman and P. Charbonneau, Mode-coupling theory, J. Stat. Mech. (2005) P05013.
[36] D. Mao, D. Chowdhury, and T. Senthil, Slow scrambling and hidden integrability in a random rotor model, Phys. Rev. B **102**, 094306 (2020).
[37] G. Cheng and B. Swingle, Chaos in a quantum rotor model, arXiv:1901.10446.
[38] J. Ye, S. Sachdev, and N. Read, Solvable Spin Glass of Quantum Rotors, Phys. Rev. Lett. **70**, 4011 (1993).
[39] J. M. Kosterlitz, D. J. Thouless, and R. C. Jones, Spherical Model of a Spin-Glass, Phys. Rev. Lett. **36**, 1217 (1976).
[40] T. Scaffidi and E. Altman, Chaos in a classical limit of the Sachdev-Ye-Kitaev model, Phys. Rev. B **100**, 155128 (2019).
[41] S. J. Thomson, P. Urbani, and M. Schiró, Quantum Quenches in Isolated Quantum Glasses Out of Equilibrium, Phys. Rev. Lett. **125**, 120602 (2020).
[42] See Supplemental Material at http://link.aps.org/supplemental/10.1103/PhysRevLett.128.115302 for additional details of imaginary and real-time path integrals for quantum p-spin glass, derivativations of the saddle-point equations, and analysis of spectral fuctions, out-of-time-order correlator (OTOC) and Lyapunov exponent in the spin glass and paramagnetic phases.
[43] The classical limit $\Gamma \to 0$ can be also taken by $M \to \infty$ with fixed $\hbar$, but this limit trivially corresponds to infinitely massive particle and there is no dynamics in the classical limit. For all our results, we calculate λ_L (in units of $J/\hbar$) as a function of Γ and obtain λ_L in units of J by dividing with $\sqrt{\Gamma J}$ for $M = 1$. The $\hbar \to 0$ limit, unlike the $M \to \infty$ limit, leads to nontrivial classical dynamics, e.g., two-step glassy relaxation in the PM phase.
[44] J. Maldacena and D. Stanford, Remarks on the Sachdev-Ye-Kitaev model, Phys. Rev. D **94**, 106002 (2016).
[45] A. Houghton, S. Jain, and A. P. Young, Role of initial conditions in the mean-field theory of spin-glass dynamics, Phys. Rev. B **28**, 2630 (1983).
[46] L. F. Cugliandolo, G. S. Lozano, and N. Nessi, Role of initial conditions in the dynamics of quantum glassy systems, J. Stat. Mech. (2019) 023301.
[47] D. Stanford, Many-body chaos at weak coupling, J. High Energy Phys. 10 (2016) 009.
[48] J. Kim and X. Cao, Comment on "Chaotic-Integrable Transition in the Sachdev-Ye-Kitaev Model", Phys. Rev. Lett. **126**, 109101 (2021).
[49] J. Kim, X. Cao, and E. Altman, Scrambling versus relaxation in Fermi and non-Fermi liquids, Phys. Rev. B **102**, 085134 (2020).
[50] G. Pöschl and E. Teller, Bemerkungen zur Quantenmechanik des anharmonischen Oszillators, Z. Phys. **83**, 143 (1933).
[51] S. Sastry, Lyapunov Spectra, Instantaneous Normal Mode Spectra, and Relaxation in the Lennard-Jones Liquid, Phys. Rev. Lett. **76**, 3738 (1996).
[52] T. Anous and F. M. Haehl, The quantum p-spin glass model: A user manual for holographers, J. Stat. Mech. (2021) 113101.